

The use of open boundaries in stochastic hydrodynamic models of nucleation

James F. Lutsko*

Center for Nonlinear Phenomena and Complex Systems

CP 231 and BLU-ULB Space Research Center,

Université Libre de Bruxelles, Blvd. du Triomphe, 1050 Brussels, Belgium

Abstract

Stochastic hydrodynamics is a central tool in the study of first order phase transitions at a fundamental level. Combined with sophisticated free energy models, e.g. as developed in classical Density Functional Theory, complex processes such as crystallization can be modeled and information such as free energy barriers, nucleation pathways and the unstable eigenvector and eigenvalues determined. The latter are particularly interesting as they play key roles in defining the natural (unbiased) order parameter and the nucleation rate respectively. As is often the case, computational realities restrict the size of system that can be modeled and this makes it difficult to achieve experimental conditions for which the volume is effectively infinite. In this paper, the use of open boundary conditions is discussed. By using an open system, the calculations become much closer to experimental conditions however, the introduction of open boundary conditions raises a number of questions concerning the stochastic model such as whether the fluctuation-dissipation relation is preserved and whether stationary points on the free energy surface remain stationary points of the dynamics. These questions are addressed here and illustrated with calculations on realistic systems.

I. INTRODUCTION

Stochastic models are an important tool used to bridge the gap between exact, microscopic dynamics and macroscopic, observable phenomenon[1]. Historically, they have often arisen based on physical heuristics - such as the Einstein-Smolochowski description of diffusion and Landau's fluctuating hydrodynamics[2, 3]- but they can also be founded in more systematic developments based, e.g. on projection operator techniques[4–6]. The stochastic component that distinguishes them captures such effects as thermal fluctuations and interactions with small particles (e.g. a bath) which play a crucial role in diverse phenomena such as protein folding[7], the wetting transition[8, 9], the Cassie-Baxter to Wenzel transition associated with the filling of pores[10] and first order phase transitions[11]. Recently, one such model consisting of a combination of fluctuating hydrodynamics and classical Density Functional Theory (cDFT)[12, 13], called Mesoscopic Nucleation Theory (MNT)[14–16], has been used to study first order phase transitions and particularly the complex phenomenon of

* <http://www.lutsko.com>; jlutsko@ulb.be

crystallization [16, 17]. Fundamental work on the microscopic foundations of this model[18] combined with the analysis of its relation to the heuristic, macroscopic Classical Nucleation Theory (CNT)[15] - as well as to intermediate approaches such as Phase Field Theory[19] - has laid the foundations for a statistical mechanical description of the dynamics of first order nucleation in general and of crystallization in particular.

Fluctuating hydrodynamics describes the time evolution of the local densities of the conserved quantities mass, momentum and energy driven by gradients of mass, pressure, temperature and by imposed external forces plus, of course, thermal fluctuations[2, 3]. As is the case with any coarse grained model, various quantities must be approximated, even if exact microscopic expressions for them exist. A key example in the application of fluctuating hydrodynamics to phase transitions is the local pressure. In MNT, this is related to a free energy functional for which models developed in cDFT are used. The cDFT free energies are functionals of the local density and are based on rigorous results from equilibrium statistical mechanics. They accurately describe the spatial structure of inhomogeneous systems at all length scales and are thus suitable for studying crystallization in which molecular-scale inhomogeneities in the density are fundamental[20]. An important application for which it is possible to simplify the problem is that of nucleation of colloids (and macromolecules) from solution in which case it is reasonable to work in the over-damped regime. This has the advantage that the hydrodynamic description reduces to a single equation for the local density and the resulting model is recognized as a version of the Dean-Kawasaki model introduced in other contexts[21–23] and also known as stochastic Dynamical Density Functional Theory[24].

When a dense phase, such as a dense droplet or a crystal, nucleates from solution in a closed system the concentration of the solution necessarily decreases which in turn changes the characteristics (e.g. free energy barrier and nucleation rate) of the process. However, in many applications, the volumes are macroscopic and the rate of nucleation very small so that for all practical purposes, the concentration remains effectively constant. In contrast, numerical applications of MNT, as in simulations, are generally restricted to much smaller volumes and so any nucleation has a strong effect on the concentration of a closed system. For this reason, to achieve correspondence with the common experimental situation it is more practical to consider open systems in which mass is not conserved. Since MNT is based on hydrodynamics, in which mass is conserved, the most natural way to do this is via

the boundary conditions imposed on the system. The present work is an exploration of the formal and technical consequences of applying such open boundary conditions to Dean-Kawasaki type models. Three main formal issues will be addressed. First, since these models usually involve state-dependent noise, their interpretation in terms of stochastic processes is a technical, but not trivial point and it will be seen that open boundaries complicates the discussion. This is not only a mathematical issue but in fact is required so that the free energy functional used is actually the free energy of the system when it is in equilibrium. The second issue to be considered is particularly motivated by the application to nucleation and involves compatability of the dynamics with the usual predictions of cDFT. Classical DFT allows one to determine the critical cluster and properties, which plays a central role in understanding nucleation and it is reasonable to demand the the dynamic model respects these results: that is, to demand that minima and saddle points on the free energy surface are stationary states of the dynamical model. As is explained below, this is again not just a formal requirement but allows for the use of very convenient techniques in actual applications. The third and final issue is the effect of the boundaries on the calculation of unstable modes of critical clusters, which is another key quantity in the description of nucleation.

The analysis presented here is phrased in terms of the specifics of MNT although one expects that the conclusions can easily be extrapolated to other applications. For this reason, the next Section gives a brief overview of the cDFT that is the source of the free energy functionals used in the stochastic model, its particular connection to nucleation and how numeric calculations are formulated. The third section addresses the dynamics including the important constraint of the fluctuation-dissipation relation, and the way in which fixed boundaries naturally lead to the transition from a canonical free energy surface to a grand-canonical surface and the important role of the choice of discretization scheme on the formal properties of the discretized model. Section IV presents some illustrative calculations showing strengths and weaknesses of the various discretization schemes. In the final, concluding Section, the practical take-aways of the analysis are summarized.

II. CLASSICAL DFT

A. cDFT formalism

The foundations of cDFT is closely related to that of the more well-known quantum DFT but its practical development is very different[12, 13]. Like qDFT, it is formulated in terms of a local density $\rho(\mathbf{r})$, although in cDFT is the mass or number density whereas in qDFT it is the local electron density. Similarly, cDFT is based on the proof of the existence of a functional of the local density $\Omega_{\mu TV}[n; \varphi]$ which, as indicated, depends on the chemical potential μ , the temperature T , the volume V and any external field $\varphi(\mathbf{r})$ acting on the system and which has the property that it is minimized by the equilibrium density distribution $\rho^{\text{eq}}(\mathbf{r})$. Furthermore, the value of the functional evaluated at the minimum is the grand-canonical free energy, $\Omega_{\mu TV} = \Omega_{\mu TV}[\rho^{\text{eq}}; \varphi]$. If more than one density gives the same minimum, then multiple coexisting states are possible. Thus, the equilibrium density can be found by minimizing the functional. The functional Ω has the structure

$$\Omega_{\mu TV}[\rho; \varphi] = F_{TV}[\rho] + \int_V (\varphi(\mathbf{r}) - \mu) \rho(\mathbf{r}) d\mathbf{r} \quad (1)$$

where the field-independent functional $F[n]$, usually called the Helmholtz functional, is not known except for some special cases[13, 25, 26].

To determine the equilibrium state(s), one can take the functional derivative with respect to density and set it equal to zero resulting in the Euler-Lagrange equation

$$\frac{\delta F_{TV}[n]}{\delta n(\mathbf{r})} = \mu - \varphi(\mathbf{r}). \quad (2)$$

Note however that solutions to this equation are not just quasi-stable minima on the free energy surface but more generally, stationary points including unstable saddle points. In the absence of external fields and in the thermodynamic limit of very large volumes, the minima are typically either homogeneous, $\rho^{\text{eq}}(\mathbf{r}) = \bar{\rho}$, corresponding to vapor and liquid phases, or crystalline solids. Often, three or more such minima exist with the thermodynamic equilibrium state being the absolute minimum. Since the minima are stable, they divide density space into regions attracted to each minimum with the border being any two such regions being a separatrix. The lowest point on each separatrix is a saddle point or, physically, a critical cluster and these also, since they are stationary points, solve the Euler-Lagrange equation.

B. cDFT and Nucleation: finding critical clusters

Critical clusters are the key objects in studying nucleation so it is important to be able to find them. A variety of methods are available for the general problem of locating saddle points on a high-dimensional energy surface[27] and here we only mention two methods which are particularly useful for the nucleation problem. First, consider the nucleation of a condensed phase from a low density (vapor) mother phase in a system with a fixed number of particles. In this case, as clusters grow, the density of the mother phase outside the cluster decreases which causes an increase in free energy of the vapor background. At some point, a critical size is reached and, just as for the grand-canonical case, if the cluster grows slightly larger than the critical size it becomes super-critical and the free energy of the whole system is lowered. However, since the density of the background is decreasing as it grows, at some point when the cluster becomes sufficiently large, a stable equilibrium is reached - the limit would have to be sometime before the background density reaches zero. So for the constant-mass system, there is a stable cluster larger than the critical cluster. Now, if the constraint of constant mass is removed - in other words, if we open the system - this stable cluster becomes unstable because it can grow without decreasing the background density. Thus, the stable cluster for the closed system is a saddle point - i.e. a critical cluster - for the open system. This intuition can easily be formalized[20]. One can minimize the free energy functional at constant particle number via the introduction of a Lagrange multiplier λ , one minimizes the Lagrangian

$$L[\rho] = \Omega_{\mu' TV}[\rho; \varphi] + \lambda \left(N - \int_V \rho(\mathbf{r}) d\mathbf{r} \right), \quad (3)$$

where μ' can be anything, giving the Euler-Lagrange equations

$$\begin{aligned} \frac{\delta F_{TV}[\rho]}{\delta \rho(\mathbf{r})} &= \mu' - \varphi(\mathbf{r}) - \lambda \\ \int_V \rho(\mathbf{r}) d\mathbf{r} &= N \end{aligned} \quad (4)$$

to be solved simultaneously for λ and $\rho(\mathbf{r})$. If a cluster-like solution is found, and in practice this is generally the case if starting from any cluster-like initial density, then comparing the first of Eq.(4) to the open-system Euler-Lagrange equation (2), one sees that the solution to the former is also a solution to the latter for the chemical potential $\mu = \mu' - \lambda$. This method has the advantage that the same techniques (and code) used to find stable solutions

to the open-system Euler-Lagrange equation can be re-used to find critical clusters. The disadvantage is that one does not control any properties - such as the chemical potential, background density or critical size - directly.

A second method, also used in the present work, is to minimize the magnitude of the forces. Specifically, instead of minimizing $L[n]$ for a closed system, one can minimize the squared forces by solving

$$0 = \frac{\delta}{\delta \rho(\mathbf{r})} \int_V \left(\frac{\delta L[\rho]}{\delta \rho(\mathbf{r}')} \right)^2 d\mathbf{r}' = 2 \int_V \left(\frac{\delta L[n]}{\delta \rho(\mathbf{r}')} \right) \left(\frac{\delta^2 L[\rho]}{\delta \rho(\mathbf{r}') \delta \rho(\mathbf{r})} \right) d\mathbf{r}' \quad (5)$$

provided that the right hand side can be conveniently evaluated. This turns out to be the case for the cDFT functionals used in MNT, see below, so that this is a practical alternative to the previous method which has the advantage that it can be directly performed on an open system. While any stationary density distribution is clearly a minimum of the functional, the disadvantage is that one must start with some sort of "reasonable" guess or risk falling down to a trivial solution. For the example of droplet nucleation discussed below, it is the case that even quite crude capillary approximations to a critical cluster are generally good enough starting points.

C. Discretized model

The equations will be discretized on a cubic grid with lattice points $\mathbf{r}_{\mathbf{I}} = \Delta \mathbf{I}_a \hat{\mathbf{e}}_a$ where Δ is the lattice constant, $\hat{\mathbf{e}}_a$ for $a = x, y, z$ are the cartesian directions and the superindex $\mathbf{I} = (I_x, I_y, I_z)$ with $0 \leq I_a < N_a - 1$. In the following, these are combined so that e.g. $\mathbf{I} \pm \hat{\mathbf{e}}_x \equiv (I_x \pm 1, I_y, I_z)$. The density at lattice point $\mathbf{r}_{\mathbf{I}}$ is written as $\rho_{\mathbf{I}} \equiv \rho(\mathbf{r}_{\mathbf{I}})$. There is often need in the following to refer to the collection of all of the discrete density variables so these will be denoted collectively as ρ . Periodic boundaries are assumed in all calculations of the free energy functionals with periodicity $\mathbf{N} = (N_x, N_y, N_z)$ so that $\rho_{\mathbf{I}} = \rho_{\mathbf{I} + N_a \hat{\mathbf{e}}_a}$ for $a \in (x, y, z)$. This means that, with no other constraints, there are a total of $N_x \times N_y \times N_z$ independent values of the density and all sums are over all of these components. The free energy functional then becomes a function of the variables $\rho_{\mathbf{I}}, \Omega_{\mu TV}[\rho; \varphi] \rightarrow \Omega_{\mu TV}(\rho; \varphi)$, e.g.

$$\int_V \rho(\mathbf{r}) \varphi(\mathbf{r}) d\mathbf{r} \rightarrow \sum_{\mathbf{I} \in \mathcal{V}} \rho_{\mathbf{I}} \varphi_{\mathbf{I}} \Delta^3$$

where \mathcal{V} is the set of all valid indices, $(0, 0, 0)$ to $(N_x - 1, N_y - 1, N_z - 1)$, and functional derivatives become ordinary derivatives

$$\frac{\delta}{\delta \rho(\mathbf{r})} \rightarrow \frac{1}{\Delta^3} \frac{\partial}{\partial \rho_{\mathbf{I}}}. \quad (6)$$

Details of the specific cDFT model used in this work have been given elsewhere[28]. In brief, taking the simplest case as illustration, the Helmholtz functional for a single-species system of molecules interacting via the pair potential $v(\mathbf{r}_1 - \mathbf{r}_2)$, is written as the sum of three contributions, $F_{TV}[\rho] = F_{TV}^{(\text{id})}[\rho] + F_{TV}^{(\text{HS})}[\rho] + F_{TV}^{(\text{mf})}[\rho]$. The ideal gas contribution is

$$F_{TV}^{(\text{id})}[\rho] = \sum_{\mathbf{I} \in \mathcal{V}} (\rho_{\mathbf{I}} \ln(\rho_{\mathbf{I}} \Lambda^3) - \rho_{\mathbf{I}}) \Delta^3, \quad (7)$$

where Λ is the thermal wavelength and the hard-sphere contribution is

$$F_{TV}^{(\text{HS})}[\rho] = \sum_{\mathbf{I} \in \mathcal{V}} \Phi(\eta^{(1)}, \eta^{(2)} \dots) \Delta^3, \quad \eta_{\mathbf{I}}^{(\alpha)}(\rho) = \sum_{\mathbf{J} \in \mathcal{V}} w_{\mathbf{I}-\mathbf{J}}^{(\alpha)} \rho_{\mathbf{J}} \Delta^3 \quad (8)$$

where Φ is a function of the so-called fundamental measures, $\eta_{\mathbf{I}}^{(\alpha)}$, which in turn are expressed in terms of convolutions of the density with weights $w_{\mathbf{I}-\mathbf{J}}^{(\alpha)}$ [13, 29, 30] (the present calculations use the explicitly stable fundamental measure theory[25]). The final contribution is a mean-field term

$$F_{TV}^{(\text{mf})}[\rho] = \frac{1}{2} \sum_{\mathbf{I}, \mathbf{J} \in \mathcal{V}} \rho_{\mathbf{I}} \rho_{\mathbf{J}} v_{\mathbf{I}-\mathbf{J}}^{(\text{att})} \Delta^6 \quad (9)$$

where $v_{\mathbf{I}-\mathbf{J}}^{(\text{att})}$ is the discretized form of the attractive part of the pair potential describing molecular interactions. Note that the mean field term, as well as the fundamental measures, are convolutions and so can be efficiently evaluated with fast Fourier transforms (FFTs). The derivative of the free energy with respect to the density is

$$\frac{\partial F(\rho)}{\partial \rho_{\mathbf{I}}} = \ln(\rho_{\mathbf{I}} \Lambda^3) \Delta^3 + \sum_{\mathbf{J} \in \mathcal{V}} \sum_{\alpha} \frac{\partial \Phi}{\partial \eta_{\mathbf{J}}^{(\alpha)}} w_{\mathbf{J}-\mathbf{I}}^{(\alpha)} \Delta^6 + \sum_{\mathbf{J} \in \mathcal{V}} \rho_{\mathbf{J}} v_{\mathbf{I}-\mathbf{J}}^{(\text{att})} \Delta^6 \quad (10)$$

and

$$\frac{\partial F(\rho)}{\partial \rho_{\mathbf{I}} \partial \rho_{\mathbf{J}}} = \frac{\Delta^3}{\rho_{\mathbf{I}}} + \sum_{\mathbf{K}, \mathbf{L} \in \mathcal{V}} \sum_{\alpha, \gamma} \frac{\partial^2 \Phi}{\partial \eta_{\mathbf{K}}^{(\alpha)} \partial \eta_{\mathbf{L}}^{(\gamma)}} w_{\mathbf{K}-\mathbf{I}}^{(\alpha)} w_{\mathbf{L}-\mathbf{J}}^{(\gamma)} \Delta^9 + v_{\mathbf{I}-\mathbf{J}}^{(\text{att})} \Delta^6 \quad (11)$$

which can, again, be efficiently evaluated with discrete FFTs.

III. DYNAMICAL FORMALISM

A. Stochastic dynamics and fluctuation-dissipation relation

The stochastic differential equation governing the dynamics of over-damped MNT is

$$\frac{\partial}{\partial t}\rho_t(\mathbf{r}) = D\nabla \cdot \rho_t(\mathbf{r})\nabla \frac{\delta\beta F[n]}{\delta n(\mathbf{r})}\bigg|_{n(\mathbf{r})=\rho_t(\mathbf{r})} + \nabla \cdot \sqrt{2D\rho_t(\mathbf{r})} \xi(\mathbf{r}, t) \quad (12)$$

where D is the tracer diffusion constant, the square brackets indicate a functional dependence and δ indicates a functional derivative. The free energy $F[\rho]$ is a functional of the local density and $\xi(\mathbf{r}, t)$ represents gaussian white noise, so $\langle \xi(\mathbf{r}, t)\xi(\mathbf{r}', t') \rangle = \delta(\mathbf{r} - \mathbf{r}')\delta(t - t')$. This can be expressed in a more abstract, but useful, form as

$$\frac{\partial}{\partial t}\rho_t(\mathbf{r}) = -D \int_V g(\mathbf{r}, \mathbf{r}'; [\rho_t]) \frac{\delta\beta F[n]}{\delta n(\mathbf{r}')} \bigg|_{n(\mathbf{r}')=\rho_t(\mathbf{r}')} d\mathbf{r}' + \sqrt{D} \int_V \sum_{a \in \{x, y, z\}} q_a(\mathbf{r}, \mathbf{r}'; [\rho_t]) \xi_a(\mathbf{r}', t) d\mathbf{r}' \quad (13)$$

where V is the integration volume and

$$\begin{aligned} g(\mathbf{r}, \mathbf{r}'; [\rho_t]) &= -\nabla \cdot \rho_t(\mathbf{r})\nabla \delta(\mathbf{r} - \mathbf{r}') \\ \mathbf{q}(\mathbf{r}, \mathbf{r}'; [\rho_t]) &= \nabla \sqrt{2\rho_t(\mathbf{r})} \delta(\mathbf{r} - \mathbf{r}'). \end{aligned} \quad (14)$$

It is shown in the Appendix that, for a rectilinear system with periodic boundaries, these operators obey a fluctuation-dissipation relation,

$$\int_V \mathbf{q}(\mathbf{r}, \mathbf{r}'; [\rho]) \cdot \mathbf{q}(\mathbf{r}'', \mathbf{r}'; [\rho]) d\mathbf{r}' = 2g(\mathbf{r}, \mathbf{r}''; [\rho]), \quad (15)$$

which assures that the operator $g(\mathbf{r}, \mathbf{r}''; [\rho])$ is positive semi-definite.

A stationary state of the deterministic part of the dynamics is a density distribution, ρ^{stat} for which $\nabla \cdot \rho(\mathbf{r})\nabla \frac{\delta F[\rho]}{\delta \rho(\mathbf{r})}\bigg|_{\rho^{\text{stat}}(\mathbf{r})} = 0$. In practice, the most important such states for a system with periodic boundaries are those for which $\frac{\delta F[\rho]}{\delta \rho(\mathbf{r})}\bigg|_{\rho^{\text{stat}}(\mathbf{r})} = \lambda$ where λ is a constant. It proves convenient - indeed, crucial - for the case of open systems to modify the force as $F[\rho] \rightarrow \Omega[\rho; \lambda] \equiv F[\rho] - \lambda N[\rho]$ where the total number of particles in the **computational volume** is $N[\rho] \equiv \int_V \rho(\mathbf{r}) d\mathbf{r}$. This clearly makes no difference for periodic systems since translational invariance means that the gradients give zero acting on the constant λ . However, for open systems in which we freeze the density on the boundaries, this term will be critical in preserving the usual stationary states, as will be made evident below.

B. Discretized equations

The fact that the right hand side of Eq.(12) is a total gradient implies that mass is conserved when periodic boundaries are used and so we refer to this as a **closed system**. To model an **open system**, we will fix the densities on the border to a given value, ρ_B , in which case mass is not conserved. In the following, we define \mathcal{V} to be the set of all lattice points, $\partial\mathcal{V}$ to be the lattice points on the boundary and so the interior, non-boundary, points are $\mathcal{V} - \partial\mathcal{V}$. Finally, we let \mathcal{D} be the set of *dynamical* points meaning those points for which the density is a dynamical variable that can change in time. So, $\mathcal{D} = \mathcal{V}$ for periodic boundaries (closed systems) and $\mathcal{D} = \mathcal{V} - \partial\mathcal{V}$ for fixed boundaries (open systems).

Differential operators, like ∇ will be discretized using either forward or central differences. The operator $\nabla \cdot \rho_t(\mathbf{R})\nabla \rightarrow g_{\mathbf{IJ}}(\rho_t)$ where the form of the matrix $g_{\mathbf{IJ}}(\rho_t)$ will be given explicitly below. The discretized dynamical equations can then be written as

$$\frac{\partial \rho_{t\mathbf{I}}}{\partial t} = -D \sum_{\mathbf{J} \in \mathcal{D}} g_{\mathbf{IJ}}(\rho_t) \frac{\partial \beta F(\rho_t)}{\partial \Delta^3 \rho_{t\mathbf{J}}} + \sqrt{\frac{2D}{\Delta^3}} \sum_{a \in \{x,y,z\}} \sum_{\mathbf{J} \in \mathcal{V}} q_{\mathbf{IJ}a}(\rho_t) \xi_{t\mathbf{J}a}, \quad \mathbf{I} \in \mathcal{D}, \quad \langle \xi_{t\mathbf{I}a} \xi_{t'\mathbf{J}b} \rangle = \delta_{ab} \delta_{\mathbf{IJ}} \delta(t - t') \quad (16)$$

or

$$\frac{\partial \rho_{t\mathbf{I}}}{\partial t} = -D \sum_{\mathbf{J} \in \mathcal{D}} g_{\mathbf{IJ}}(\rho_t) \frac{1}{\Delta^3} \beta F_{\mathbf{J}}(\rho_t; \lambda) + \sqrt{\frac{2D}{\Delta^3}} \sum_{a \in \{x,y,z\}} \sum_{\mathbf{J} \in \mathcal{V}} q_{\mathbf{IJ}a}(\rho_t) \xi_{t\mathbf{J}a}, \quad \mathbf{I} \in \mathcal{D} \quad (17)$$

where here and in the following the compact notation

$$\begin{aligned} \beta F_{\mathbf{J}}(\rho) &\equiv \frac{\partial \beta F(\rho)}{\partial \rho_{\mathbf{J}}}, \quad \mathbf{J} \in \mathcal{D} \\ \beta F_{\mathbf{IJ}}(\rho) &\equiv \frac{\partial^2 \beta F(\rho)}{\partial \rho_{\mathbf{I}} \partial \rho_{\mathbf{J}}}, \quad \mathbf{J} \in \mathcal{D} \end{aligned} \quad (18)$$

is used. The sums over the noise terms deliberately include all points, and not just the dynamical points, for reasons explained below. The fluctuation-dissipation relation becomes

$$g_{\mathbf{IJ}}(\rho) = \sum_{a \in \{x,y,z\}} \sum_{\mathbf{K} \in \mathcal{V}} q_{\mathbf{IK}a} q_{\mathbf{JK}a} \quad (19)$$

and demanding that any discretization of the model satisfy this relation is crucial since it assures that the matrix $g(\rho)$ is positive semidefinite and this in turn is necessary so as not to introduce spurious unstable modes into the dynamics.

We recall that in the case of state-dependent noise, as is the case here, the stochastic differential equation must be supplemented with an *interpretation*. In the case of a discretized

time variable, the interpretation specifies whether the noise amplitude is to be evaluated at the beginning of the time step (the Ito interpretation), at the middle of the time step (the Stratonovich interpretation) or the end of the time-step (the anti-Ito interpretation). The latter two result in semi-implicit and implicit discretization schemes, respectively, and - unlike the case of the deterministic term - do not give identical results in the limit that the time-step goes to zero. A practical consequence is the form of the Fokker-Planck equation for the probability that the system has state values ρ at time t , $P(\rho, t)$ which, in the present case, is

$$\frac{\partial}{\partial t} P_t(\rho) = - \sum_{\mathbf{I}, \mathbf{J} \in \mathcal{D}} \frac{\partial}{\partial \rho_{\mathbf{I}}} \left(D g_{\mathbf{I}\mathbf{J}}(\rho) \beta F_{\mathbf{J}}(\rho) + \sqrt{\frac{2D}{\Delta^3}} \left\{ \sum_a \sum_{\mathbf{K} \in \mathcal{V}} q_{\mathbf{I}\mathbf{K}a}(\rho) \frac{\partial}{\partial \rho_{\mathbf{J}}} q_{\mathbf{J}\mathbf{K}a}(\rho) \right\} \right) P_t(\rho) \quad (20)$$

for the three cases (going from top to bottom), respectively. The Ito and Stratonovich interpretations are equivalent if and only if

$$\sum_{\mathbf{J} \in \mathcal{D}} \sum_{a \in \{x, y, z\}} \sum_{\mathbf{K} \in \mathcal{V}} \left(\frac{\partial}{\partial \rho_{\mathbf{J}}} q_{\mathbf{I}\mathbf{K}a}(\rho) \right) q_{\mathbf{J}\mathbf{K}a}(\rho) = 0 \quad (21)$$

and the Stratonovich and anti-Ito are the same if

$$\sum_{\mathbf{J} \in \mathcal{D}} \sum_{a \in \{x, y, z\}} \sum_{\mathbf{K} \in \mathcal{V}} q_{\mathbf{I}\mathbf{K}a}(\rho) \left(\frac{\partial}{\partial \rho_{\mathbf{J}}} q_{\mathbf{J}\mathbf{K}a}(\rho) \right) = 0 \quad (22)$$

In a well-known contribution to the theory of fluctuating hydrodynamics, from which this over-damped dynamics is derived, it was shown that for closed systems, discretization with centered finite differences resulted in Ito-Stratonovich equivalence[31]. One goal below is to explore this for an open system. Finally, note from Eq. (20) that for the anti-Ito interpretation, stationary distributions (i.e. setting $\frac{\partial}{\partial t} P_t(\rho) = 0$) include

$$P(\rho) = A e^{-\beta F(\rho)}, \quad (23)$$

where A is any constant, as expected. This is a strong motivation for preferring models that are the same in all statistical interpretations.

C. Central differences

Writing the gradient operator as $\nabla_a \rightarrow \frac{1}{2\Delta} \left(\delta_{\mathbf{K}}^{\mathbf{I}+\hat{\mathbf{e}}_{(a)}} - \delta_{\mathbf{K}}^{\mathbf{I}-\hat{\mathbf{e}}_{(a)}} \right)$ results in the discretization

$$q_{\mathbf{IK}a}(\rho) = \frac{1}{2\Delta} \left(\delta_{\mathbf{I}+\hat{\mathbf{e}}_{(a)}\mathbf{K}} - \delta_{\mathbf{I}-\hat{\mathbf{e}}_{(a)}\mathbf{K}} \right) \sqrt{\rho_{\mathbf{K}}}, \quad \mathbf{I} \in \mathcal{D}, \mathbf{K} \in \mathcal{V} \quad (24)$$

giving, via the fluctuation-dissipation relation

$$g^{\mathbf{IJ}} = \sum_{a \in \{x,y,z\}} \sum_{\mathbf{K} \in \mathcal{V}} q_{\mathbf{IK}a}(\rho) q_{\mathbf{JK}a}(\rho) = -\frac{1}{4\Delta^2} \sum_{a \in \{x,y,z\}} \left\{ \rho_{\mathbf{I}+\hat{\mathbf{e}}_{(a)}} \left(\delta_{\mathbf{I}+2\hat{\mathbf{e}}_{(a)}\mathbf{J}} - \delta_{\mathbf{IJ}} \right) - \rho_{\mathbf{I}-\hat{\mathbf{e}}_{(a)}} \left(\delta_{\mathbf{IJ}} - \delta_{\mathbf{I}-2\hat{\mathbf{e}}_{(a)}\mathbf{J}} \right) \right\}, \quad \mathbf{I}, \mathbf{J} \in \mathcal{D} \quad (25)$$

Using the reverse mapping $f_{\mathbf{I} \pm 2\hat{\mathbf{e}}_{(a)}} \rightarrow f(\mathbf{r}_{\mathbf{I}} \pm 2\Delta\hat{\mathbf{e}}_{(a)})$, etc., it is straightforward to show that away from the boundaries (in the sense that $\mathbf{I}, \mathbf{I} \pm 2\hat{\mathbf{e}}_{(a)} \in \mathcal{D}$),

$$\lim_{\Delta \rightarrow 0} \left(\sum_{\mathbf{J} \in \mathcal{D}} g_{\mathbf{IJ}} f_{\mathbf{J}} \right) = -(\nabla \cdot \rho(\mathbf{r}) (\nabla f(\mathbf{r})))_{\mathbf{r}_{\mathbf{I}}} \quad (26)$$

as required.

For an arbitrary vector $f_{\mathbf{I}}$,

$$v_{\mathbf{I}} \equiv \sum_{\mathbf{J} \in \mathcal{D}} g_{\mathbf{IJ}} f_{\mathbf{J}} = -\frac{1}{4\Delta^2} \sum_{a \in \{x,y,z\}} \left\{ \rho_{\mathbf{I}+\hat{\mathbf{e}}_{(a)}} \left(\tilde{f}_{\mathbf{I}+2\hat{\mathbf{e}}_{(a)}} - \tilde{f}_{\mathbf{I}} \right) - \rho_{\mathbf{I}-\hat{\mathbf{e}}_{(a)}} \left(\tilde{f}_{\mathbf{I}} - \tilde{f}_{\mathbf{I}-2\hat{\mathbf{e}}_{(a)}} \right) \right\}, \quad \mathbf{I} \in \mathcal{D} \quad (27)$$

where we define $\tilde{f}_{\mathbf{I}} = f_{\mathbf{I}}$ for $\mathbf{I} \in \mathcal{D}$ and $\tilde{f}_{\mathbf{I}} = 0$ for $\mathbf{I} \notin \mathcal{D}$. For open systems, for which $\mathcal{D} \neq \mathcal{V}$, this extends the vector $f_{\mathbf{I}}$ to the entire lattice in a way that gives the correct result for this sum. It is thus immediately clear that $f_{\mathbf{I}} = 1$ is a zero eigenvector of $g^{\mathbf{IJ}}$ for closed systems which is a natural consequence of the translational invariance of periodic boundaries. For open systems, when $\mathbf{I} \pm 2\hat{\mathbf{e}}_{(a)}$ falls on the boundary, $\tilde{f}_{\mathbf{I}+2\hat{\mathbf{e}}_{(a)}} = 0$ and so the constant vector is no longer an eigenvector, reflecting the breaking of translational invariance. However, in both cases, there are other eigenvectors with eigenvalue zero. To see this, consider one element of the sum on the right hand side of Eq.(27), say $a = x$. Then the other components

of the index are the same in all terms so, suppressing, those, we see that:

$$\begin{aligned}
v_1 &= -\frac{1}{4\Delta^2} \left\{ \rho_2 \left(\tilde{f}_3 - \tilde{f}_1 \right) - \rho_0 \left(\tilde{f}_1 - \tilde{f}_{N_x-1} \right) \right\} + \dots \\
v_2 &= -\frac{1}{4\Delta^2} \left\{ \rho_3 \left(\tilde{f}_4 - \tilde{f}_2 \right) - \rho_1 \left(\tilde{f}_2 \right) \right\} + \dots \\
v_3 &= -\frac{1}{4\Delta^2} \left\{ \rho_4 \left(\tilde{f}_5 - \tilde{f}_3 \right) - \rho_2 \left(\tilde{f}_3 - \tilde{f}_1 \right) \right\} + \dots \\
&\dots \\
v_{N_x-2} &= -\frac{1}{4\Delta^2} \left\{ \rho_{N_x-1} \left(-\tilde{f}_{N_x-2} \right) - \rho_{N_x-3} \left(\tilde{f}_{N_x-2} - \tilde{f}_{N_x-4} \right) \right\} + \dots \\
v_{N_x-1} &= -\frac{1}{4\Delta^2} \left\{ \rho_0 \left(\tilde{f}_1 - \tilde{f}_{N_x-1} \right) - \rho_{N_x-2} \left(\tilde{f}_{N_x-1} - \tilde{f}_{N_x-3} \right) \right\} + \dots
\end{aligned} \tag{28}$$

where the ellipses in the horizontal direction indicate the remaining terms from the sum over directions, $a = y$ and $a = z$. On the one hand, this clearly shows that the presence of the boundaries eliminates the zero-mode in which $f_{\mathbf{I}} = 1$ for all \mathbf{I} due to the missing f_0 terms in v_2 and v_{N_x-2} . In other words, the boundary conditions break the translational symmetry of the differential operators. On the other hand, if N_x is even, then the “missing” elements only occur in even-numbered components of f , so they can be avoided by setting all even-numbered components of f to zero while keeping the odd-numbered components equal to a constant (e.g. 1). Thus, a spurious zero-mode exists and its effect on the eigenvectors is clear in the examples below.

It follows from all of this that for a closed system, $F_{\mathbf{I}} = \lambda\Delta^3$ is a stationary state for any constant λ but for open systems this only holds if $\lambda = 0$. In order to preserve the correspondence between stationary points on the free energy surface and stationary states of the dynamics, consider the effect of applying an external one-body potential $\phi(\mathbf{r})$ on the system, which modifies the free energy as $F[\rho; \phi] = F[\rho] + \int_V \rho(\mathbf{r}) \phi(\mathbf{r}) d\mathbf{r}$ and so $F(\rho) \rightarrow F(\rho) + \sum_{\mathbf{I} \in \mathcal{D}} \rho_{\mathbf{I}} \phi_{\mathbf{I}} \Delta^3$. Then, the forces become $F_{\mathbf{I}}(\rho, \phi) = F_{\mathbf{I}}(\rho) + \phi_{\mathbf{I}} \Delta^3$ so that for the particular choice $\phi_{\mathbf{I}} = -\lambda$, a stationary state $F_{\mathbf{I}}(\rho) = \lambda\Delta^3$ corresponds to $F_{\mathbf{I}}(\rho, \phi) = 0$ giving a stationary state for both open and closed systems. Of course, $F[\rho, \phi] = F[\rho] - \lambda \int_V \rho(\mathbf{r}) d\mathbf{r}$ is recognized as the grand-canonical free energy and so one could say that in order to preserve the correspondence between stationary states in the open and closed cases of finite systems, one is led naturally to replace the canonical free energy $F[\rho]$ by the grand canonical $\Omega[\rho; \lambda] = F[\rho] - \lambda \int_V \rho(\mathbf{r}) d\mathbf{r}$ when moving from the closed to the open system.

Ito-Stratonovich equivalence can be directly verified with the simple calculation

$$\begin{aligned}
\left(\frac{\partial}{\partial \rho_{\mathbf{J}}} q_{\mathbf{I}(\mathbf{K}_a)}(\rho) \right) q_{\mathbf{J}(\mathbf{K}_a)}(\rho) &= \frac{1}{4\Delta^2} \sum_{\mathbf{J} \in \mathcal{D}} \sum_{a \in \{x,y,z\}} \sum_{\mathbf{K} \in \mathcal{V}} \left(\delta_{\mathbf{I}+\hat{\mathbf{e}}_{(a)}\mathbf{K}} - \delta_{\mathbf{I}-\hat{\mathbf{e}}_{(a)}\mathbf{K}} \right) \frac{\partial \sqrt{\rho_{\mathbf{K}}}}{\partial \rho_{\mathbf{J}}} \left(\delta_{\mathbf{J}+\hat{\mathbf{e}}_{(a)}\mathbf{K}} - \delta_{\mathbf{J}-\hat{\mathbf{e}}_{(a)}\mathbf{K}} \right) \sqrt{\rho_{\mathbf{K}}}, \quad \mathbf{I} \in \mathcal{D} \\
&= \frac{1}{8\Delta^2} \sum_{\mathbf{J} \in \mathcal{D}} \sum_{a \in \{x,y,z\}} \sum_{\mathbf{K} \in \mathcal{V}} \left(\delta_{\mathbf{I}+\hat{\mathbf{e}}_{(a)}\mathbf{K}} - \delta_{\mathbf{I}-\hat{\mathbf{e}}_{(a)}\mathbf{K}} \right) \delta_{\mathbf{J}\mathbf{K}} \left(\delta_{\mathbf{J}+\hat{\mathbf{e}}_{(a)}\mathbf{K}} - \delta_{\mathbf{J}-\hat{\mathbf{e}}_{(a)}\mathbf{K}} \right) \\
&= \frac{1}{8\Delta^2} \sum_{\mathbf{J} \in \mathcal{D}} \sum_{a \in \{x,y,z\}} \left(\delta_{\mathbf{I}+\hat{\mathbf{e}}_{(a)}\mathbf{J}} - \delta_{\mathbf{I}-\hat{\mathbf{e}}_{(a)}\mathbf{J}} \right) \left(\delta_{\mathbf{J}+\hat{\mathbf{e}}_{(a)}\mathbf{J}} - \delta_{\mathbf{J}-\hat{\mathbf{e}}_{(a)}\mathbf{J}} \right) \\
&= 0
\end{aligned} \tag{29}$$

so the model is indeed Ito-Stratonovich equivalent. Furthermore, in exactly the same way, one finds that

$$\sum_{\mathbf{J} \in \mathcal{D}} q_{\mathbf{I}(\mathbf{K}_a)}(\rho) \frac{\partial}{\partial \rho_{\mathbf{J}}} q_{\mathbf{J}(\mathbf{K}_a)}(\rho) = 0 \tag{30}$$

so Stratonovich-anti-Ito equivalence also holds. Thus, all interpretations of the stochastic differential equation are equivalent.

D. Forward differences scheme A (FWD-A)

One obvious drawback of the central-differences scheme is the presence of the spurious zero-modes discussed above which breaks the correspondence between stationary states of the dynamics and the free energy. An alternative is the use of forward differences such as $\nabla_a \rightarrow \frac{1}{\Delta} \left(\delta_{\mathbf{KI}+\hat{\mathbf{e}}_{(a)}} - \delta_{\mathbf{KI}} \right)$ so that

$$q_{a\mathbf{IK}}(\rho) = \frac{1}{\Delta} \left(\delta_{\mathbf{KI}+\hat{\mathbf{e}}_{(a)}} - \delta_{\mathbf{KI}} \right) \sqrt{\rho_{\mathbf{K}}}, \quad \mathbf{I} \in \mathcal{D}, \mathbf{K} \in \mathcal{V} \tag{31}$$

and

$$g_{\mathbf{IJ}}(\rho) = -\frac{1}{\Delta^2} \sum_{a \in \{x,y,z\}} \left(\rho_{\mathbf{I}+\hat{\mathbf{e}}_{(a)}} \left(\delta_{\mathbf{I}+\hat{\mathbf{e}}_{(a)}\mathbf{J}} - \delta_{\mathbf{IJ}} \right) - \rho_{\mathbf{I}} \left(\delta_{\mathbf{IJ}} - \delta_{\mathbf{I}-\hat{\mathbf{e}}_{(a)}\mathbf{J}} \right) \right), \quad \mathbf{I}, \mathbf{J} \in \mathcal{D} \tag{32}$$

It is again easy to show that away from the boundaries

$$\sum_{\mathbf{J} \in \mathcal{D}} g_{\mathbf{IJ}}(\rho) f_{\mathbf{J}} \xrightarrow{\Delta \rightarrow 0} -(\nabla \cdot \rho(\mathbf{r}) \nabla f(\mathbf{r}))_{\mathbf{r}_{\mathbf{I}}}. \tag{33}$$

For a general vector $f_{\mathbf{J}}$, one has that

$$\sum_{\mathbf{J} \in \mathcal{D}} g_{\mathbf{IJ}}(\rho) f_{\mathbf{J}} = -\frac{1}{\Delta^2} \delta_{\mathbf{I} \pm \hat{\mathbf{e}}_{(a)} \in \mathcal{D}} \sum_{a \in \{x,y,z\}} \left(\rho_{\mathbf{I}+\hat{\mathbf{e}}_{(a)}} \left(\tilde{f}_{\mathbf{I}+\hat{\mathbf{e}}_{(a)}} - \tilde{f}_{\mathbf{I}} \right) - \rho_{\mathbf{I}} \left(\tilde{f}_{\mathbf{I}} - \tilde{f}_{\mathbf{I}-\hat{\mathbf{e}}_{(a)}} \right) \right) \tag{34}$$

so that again, the constant vector $f_{\mathbf{J}} = 1$ is a zero-eigenvector for the closed case but not for the open case while the spurious zero-eigenvector that was present for the open system with central differences is eliminated. As to stationary states, the same conclusions as for central differences apply: $F_{\mathbf{I}} = \lambda$ is a stationary state for closed systems but not for open systems whereas $\Omega_{\mathbf{I}} = 0$ is always stationary. Checking the Ito-Stratonovich equivalence condition now gives

$$\sum_{\mathbf{J} \in \mathcal{D}} \sum_{a \in \{x,y,z\}} \sum_{\mathbf{K} \in \mathcal{V}} \frac{\partial q_{a\mathbf{I}\mathbf{K}}(\rho)}{\partial \rho_{\mathbf{J}}} q_{a\mathbf{J}\mathbf{K}}(\rho) = \frac{1}{2\Delta^2} (\delta_{I_x N_x - 1} + \delta_{I_y N_y - 1} + \delta_{I_z N_z - 1}) \quad (35)$$

and so the two interpretations are no longer equivalent, although the violations are restricted to the boundary.

E. Forward differences scheme B (FWD-B)

The interpretation-dependence of the stochastic model when formulated with forward differences can be removed by using a somewhat un-natural formulation of

$$q_{\mathbf{I}(\mathbf{K}a)}(\rho) = \frac{1}{\Delta} \left(\delta_{\mathbf{I}+\hat{\mathbf{e}}_{(a)}\mathbf{K}} - \delta_{\mathbf{I}\mathbf{K}} \right) \sqrt{\rho_{\mathbf{K}+\hat{\mathbf{e}}_{(a)}}}, \quad \mathbf{I} \in \mathcal{D}, \mathbf{K} \in \mathcal{V} \quad (36)$$

giving

$$g_{\mathbf{I}\mathbf{J}}(\rho) = -\frac{1}{\Delta^2} \sum_{a \in \{x,y,z\}} \left(\rho_{\mathbf{I}+2\hat{\mathbf{e}}_{(a)}} \left(\delta_{\mathbf{I}+\hat{\mathbf{e}}_{(a)}\mathbf{J}} - \delta_{\mathbf{I}\mathbf{J}} \right) - \rho_{\mathbf{I}+\hat{\mathbf{e}}_{(a)}} \left(\delta_{\mathbf{I}\mathbf{J}} - \delta_{\mathbf{I}-\hat{\mathbf{e}}_{(a)}\mathbf{J}} \right) \right), \quad \mathbf{I}, \mathbf{J} \in \mathcal{D} \quad (37)$$

and, despite the unnatural form of the differencing scheme, one can verify that

$$\lim_{\Delta \rightarrow 0} \left(\sum_{\mathbf{J} \in \mathcal{D}} g_{\mathbf{I}\mathbf{J}} f_{\mathbf{J}} \right) = -\nabla \cdot \rho(\mathbf{r}) \nabla f(\mathbf{r})|_{\mathbf{r}_{\mathbf{I}}}. \quad (38)$$

Checking the Ito-Stratonovich condition one now finds that the anomolous force vanishes and so the interpretations are indeed equivalent. Similarly, the shifted (i.e. grand-canonical) free energy again preserves the correspondence between stationary states of the dynamics and the free energy and there are again no spurious zero modes.

IV. CALCULATIONS

A classic problem for which this model has proven central is the nucleation of first order phase transitions where understanding the dynamics of critical clusters (i.e. saddle points

on the free energy surface) is critical. Here we will use the specific case of nucleation of liquid droplets from a vapor as an example and, specifically, on the eigenvalue and eigenvector of the unstable mode which plays a key role in calculating the nucleation rate and in identifying the order parameter[16]. Besides a comparison of the effect of the different discretization schemes, we will also use the opportunity to look at the dependence of the calculated values on the lattice spacing and the size of the computational cell. For the free energy, the standard cDFT model of a hard-core contribution (based on the explicitly-stable Fundamental Measure Theory) supplemented with a mean-field contribution is used. Computational details have been described elsewhere[20, 25, 28] and will not be repeated here except to note that we use the the Lennard-Jones (LJ) interaction potential,

$$v_{LJ}(r) = 4\epsilon \left(\left(\frac{\sigma}{r} \right)_{12} - \left(\frac{\sigma}{r} \right)^6 \right) \quad (39)$$

in our calculations, modified by a cutoff at some distance r_c and a corresponding shift so that $v(r) - v(r_c)$ for $r < r_c$ and zero for larger distances.

A. Unstable Eigenvalues

As a test of the various implementations, we will use the calculation of the unstable mode for a stationary state, ρ^* , so that $F_{\mathbf{I}}(\rho^*) = \mu$ for all $\mathbf{I} \in \mathcal{V}$. Then, writing $\rho_{t\mathbf{I}} = \rho_{\mathbf{I}}^* + \delta\rho_{t\mathbf{I}}$ and linearizing, one finds

$$\frac{\partial \delta\rho_{t\mathbf{I}}}{\partial t} = -\frac{D}{\sigma^2} \sum_{\mathbf{K} \in \mathcal{D}} D_{\mathbf{IK}} \delta\rho_{t\mathbf{K}} + \sqrt{\frac{2D}{\Delta^3}} \sum_{a \in (x,y,z)} \sum_{\mathbf{J} \in \mathcal{V}} q_{\mathbf{IJ}(a)}(\rho^*) \xi_{t\mathbf{J}(a)}, \quad \mathbf{I} \in \mathcal{D} \quad (40)$$

where the dimensionless *dynamical matrix* is

$$D_{\mathbf{IK}} \equiv \frac{\sigma^2}{\Delta^3} \sum_{\mathbf{J} \in \mathcal{D}} g_{\mathbf{IJ}}(\rho^*) \beta F_{\mathbf{JK}}(\rho^*; \lambda). \quad (41)$$

In the case that ρ^* is a critical cluster (i.e. a saddle point), there is at least one unstable mode and the eigenvalue associated with this mode is a key quantity in calculating the rate of nucleation.

The Hessian of the free energy, $F_{\mathbf{IJ}}$ is a real, symmetric matrix and so its eigenvalues are all real and its left and right eigenvectors are the same. The dynamical matrix is not symmetric and so its left and right eigenvectors are different and if the left eigenvector for

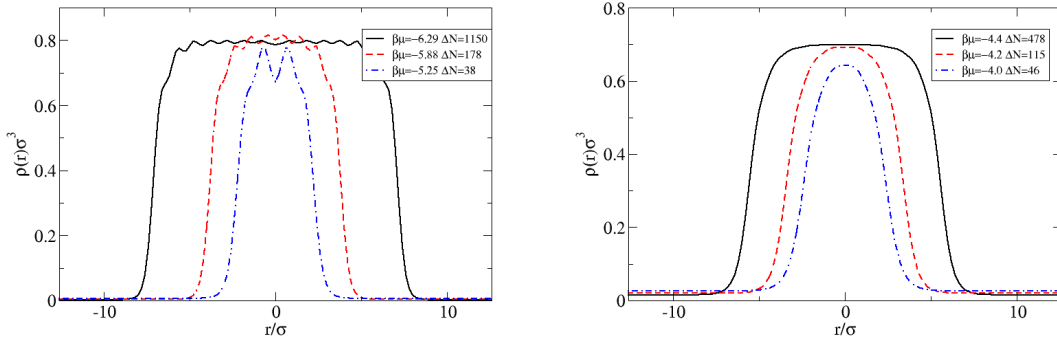


FIG. 1. The panel on the left shows critical clusters for $k_B T = 0.6\varepsilon$ and the panel on the right shows $k_B T = 0.8\varepsilon$, both with $\Delta = 0.2\sigma$.

the eigenvalue $\lambda^{(a)}$ is $u_{\mathbf{I}}^{(a)}$ then $v_{\mathbf{I}}^{(a)} \equiv \sum_{\mathbf{J} \in \mathcal{D}} g_{\mathbf{IJ}} u_{\mathbf{J}}^{(a)}$ is a right eigenvector with the same eigenvalue. It is straightforward to show that the eigenvalues are again all real (due to the fact that the dynamical matrix is the product of two real, symmetric matrices) and that the left and right eigenvectors form a biorthogonal set. For this reason, it is natural to normalize them so that $\sum_{\mathbf{J} \in \mathcal{D}} u_{\mathbf{I}}^{(a)} v_{\mathbf{I}}^{(a)} = 1$ making them bi-orthonormal.

In order to estimate the nucleation rate[16], it is necessary to determine the unstable eigenvalues of the dynamical matrix. For the systems considered here, the dimension of the space of the discretized density space ranges from 32^3 to 256^3 or from about 3×10^4 to more than 1×10^7 , with a corresponding number of eigenvalues. The dynamical matrix is generally far too large to compute or to hold in memory and diagonalization is infeasible. It is, however, possible to determine a restricted set of eigenvalues and eigenvectors. We do this using the SLEPC library[32–35]. After experimenting with many different routines, we find good results using the Jacobi-Davidson solver (EPSJD) when determining eigenpairs for the Hessian of the free energy and the Krylov-Schur solver (EPSKRYLOVSCHUR) (a variation of the Arnoldi method) for the dynamical matrix. The SLEPC library is dependent on the PETSc linear-algebra library and in both cases, the Generalized Minimal Residual method is used for solving linear systems (KSP type KSPGMRES in PETSc).

Critical clusters were created as described above based either on the correspondence between stationary states for open and closed systems or on the force method. Figure 1 shows some typical examples of the critical clusters obtained for a cubic computational cell

			$ \lambda \times 10^3$		
Δ	$\beta\Delta\Omega$	ΔN	FWD-A	FWD-B	Central
0.1	62.7	260	1.09	1.09	1.05
0.2	62.3	257	1.10	1.10	0.52
0.4	61.1	251	1.12	1.14	0.54
0.8	69.0	314	0.85	0.85	0.22

TABLE I. Sensitivity of the excess free energy, cluster mass and unstable eigenvalue to the calculational lattice spacing for $k_B T = 0.8\epsilon$ and $\beta\mu = -4.61$. The potential cutoff was $R_c = 5\sigma$ and the volume of the computational cell was held fixed at $V = (25.6\sigma)^3$ in all calculations.

with sides of length $L = 25.6\sigma$. We recall that for a cutoff of $R_c = 3\sigma$, the liquid-vapor critical temperature determined from the cDFT model is approximately $k_B T_c = 1.295\epsilon$ while the triple point is $k_B T_c = 0.798\epsilon$.

Tables I and II summarize calculations for a critical droplet in an open system using different values of the computational lattice parameter and the different discretization schemes discussed. The results using the two forward-difference schemes are in all cases very similar and are relatively independent of the lattice spacing for $\Delta \lesssim 0.4\sigma$. Physically, this is consistent with the smallest features of the density profiles being oscillations of wavelength around σ in the cooler system and gradients $d\rho\sigma^3/d(r/\sigma) \sim 0.3 - 0.5$ in the interfacial regions giving relative density variations over one computational cell of $\Delta \times d \ln \rho / dr \lesssim 0.4$ at the middle of the interfacial region. On the other hand, some variation is expected as the global properties of the clusters, such as their total excess free energy and mass, vary slightly with lattice spacing as seen in the tables. However, the central-difference results differ substantially from the forward-differences as well as showing much stronger lattice-spacing dependence, particularly at the higher temperature.

In the open system, the boundaries act as sources and sinks of density whereas inside the system, the movement of mass is conservative and diffusive. This naturally raises the question of the sensitivity of the calculations to system size (for fixed computational lattice spacing). This is illustrated in Figure 2 which shows the value of the unstable eigenvalues as functions of the system size for lattice spacing $\Delta = 0.2\sigma$. For the smallest cluster considered, containing only about 23 molecules, the eigenvalue is virtually independent of

			$ \lambda \times 10^3$		
Δ	$\beta\Delta\Omega$	ΔN	FWD-A	FWD-B	Central
0.1	21.6	38.3	5.26	5.27	4.66
0.2	21.5	38.0	5.30	5.33	4.69
0.4	21.2	37.2	5.43	5.55	4.81
0.8	21.5	38.0	4.31	4.59	3.77

TABLE II. Sensitivity of the excess free energy, cluster mass and unstable eigenvalue to the calculational lattice spacing for $k_B T = 0.6\varepsilon$ and $\beta\mu = -5.25$. The potential cutoff was $R_c = 3\sigma$ and the volume of the computational cell was held fixed at $V = (25.6\sigma)^3$ in all calculations.

box size. However, for the larger clusters, the results seem to scale with the inverse volume of the system but only vary by about a factor of 2 over the range of available box sizes (the boxes have a minimum size in order to contain the cluster and a maximum size based on computational feasibility). To give some context to the observed behaviour, we note that the clusters having excess masses of $\Delta N = 22.7, 257, 478$ and 573 have radii (based on a fit to a hyperbolic tangent profile[36]) of $3.2\sigma, 8.8\sigma, 11\sigma$ and 11.2σ , respectively.

B. Unstable eigenvectors

To understand the differences between the FWD and the CENTRAL schemes, it is useful to consider the corresponding eigenvectors. Fig.3 shows the left and right eigenvectors of the unstable mode for a small cluster at $k_B T = 0.6\varepsilon$. The right eigenvectors are quite similar for all three discretization schemes with a notable difference being that the eigenvectors for the forward schemes show some asymmetry which is presumably an echo of the un-symmetric nature of the difference scheme. The central-differences scheme is, in contrast, highly symmetric. The left eigenvectors tell a very different story: the forward-difference schemes give smooth curves which are very similar for the two schemes. In contrast, the central difference scheme shows strong oscillations on the scale of the computational lattice, presumably attributable to the partial decoupling of the even and odd sublattices as discussed above. These results are typical and for comparison, Fig. 4 shows a case at $k_B T = 0.8\varepsilon$ which is qualitatively the same.

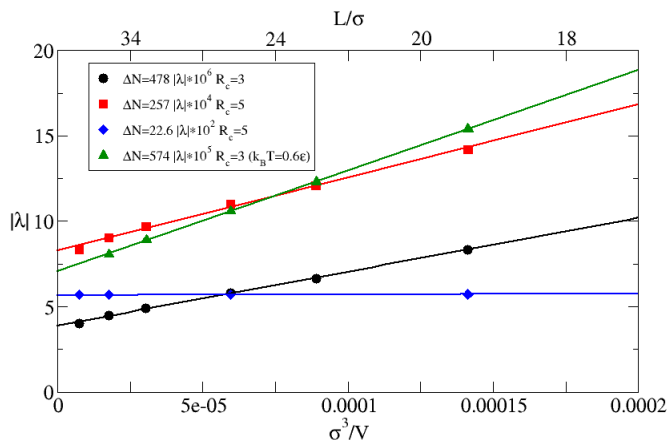


FIG. 2. Unstable eigenvalues as functions of the inverse system size as calculated using the **FWD-A** scheme. The legend gives, for each curve, the size of the critical cluster (ΔN), the scaling of the magnitude of the dimensionless (unstable) eigenvalues λ (done for display purposes) and the potential cutoff used in each calculation. All calculations were performed at $k_B T = 0.8\epsilon$ except that shown as green triangles which, as noted in the legend, was done for $k_B T = 0.6\epsilon$. The scale below the graph shows the abscissa in terms of the volume of the cubic computational cell and that above the graph shows it as the length of the computational cell's sides.

V. CONCLUSIONS

Our results show that the Dean-Kawasaki type model, at least as used in the description of nucleation, can be modified to account for open boundaries by fixing the value of the dynamical variables on the boundary. However, this raises various secondary issues which must be accounted for, namely:

- The free energy that drives the dynamics must be changed from a canonical form, applicable to systems with fixed number of particles, to a grand-canonical form in order to preserve the stationary states which are expected to be the same in both cases.
- The fixed boundaries mean that Ito-Stratonovich equivalence is sometimes violated at the boundaries, depending on the discretization scheme. Central differences and specially constructed forward-difference schemes maintain the equivalence but some natural choices do not.

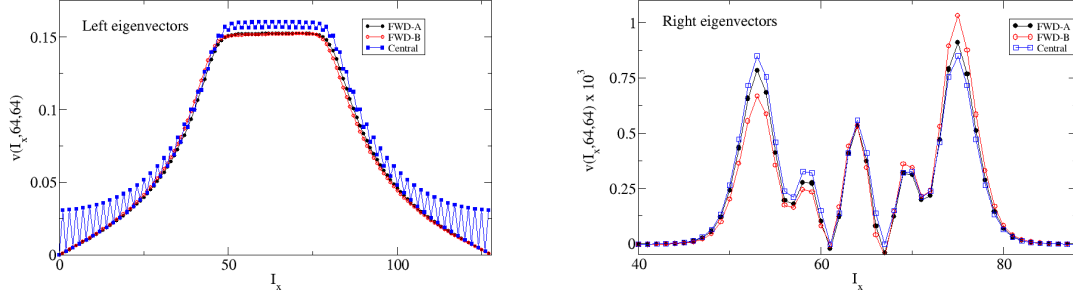


FIG. 3. Left and right eigenvectors for $k_B T = 0.6\epsilon$, $\beta\mu = -5.25$ and $\Delta = 0.2\sigma$ for the three schemes. The computational cell has 128 lattice points in each direction and the figure shows a slice through the volume that characterizes the (approximately) spherically symmetric eigenvectors.

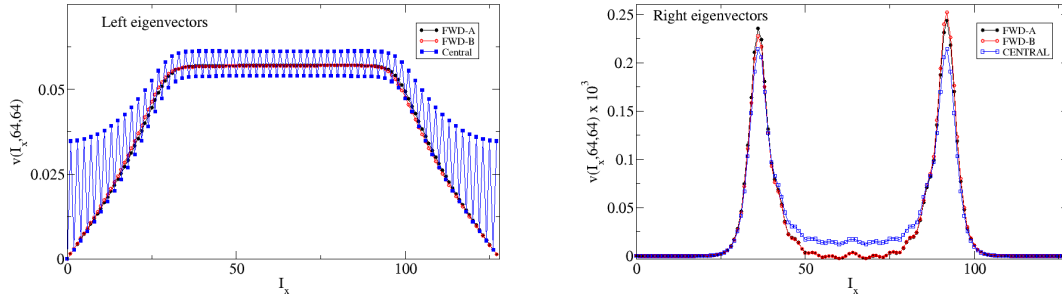


FIG. 4. Left and right eigenvectors for $k_B T = 0.8\epsilon$, $\beta\mu = -4.4$ and $\Delta = 0.2\sigma$ for the three schemes. The computational cell has 128 lattice points in each direction and the figure shows a slice through the volume that characterizes the (approximately) spherically symmetric eigenvectors.

- Central differences give a partial decoupling of the even and odd lattices with the result that a spurious zero-eigenvalue mode appears. This is avoided with the forward schemes.

As an illustration, the various schemes described here were used to calculate the unstable eigenvalue for a droplet nucleating from a vapor phase. The forward schemes showed relatively weak dependence on the lattice spacing while the central difference scheme was much more sensitive. Furthermore, the left eigenvectors of the central scheme showed spurious oscillations on the scale of the computational lattice spacing that one assumes is due to the decoupling of the lattices. Taken together, these results suggest that either of the for-

ward difference schemes could be used in practical calculations but the specially constructed FWD2 has the best formal properties of the three schemes examined.

Finally, the present analysis was performed for the Kawasaki-Dean dynamics that results from the over-damping of the full fluctuating hydrodynamics model. The present results suggest that it should be possible to formulate an open-system version of the latter along similar lines although a detailed analysis would be necessary to be sure.

ACKNOWLEDGMENTS

This work was supported by the European Space Agency (ESA) and the Belgian Federal Science Policy Office (BELSPO) in the framework of the PRODEX Programme, Contract No. ESA AO-2004-070.

-
- [1] C. W. Gardiner, *Handbook of Stochastic Methods*, 3ed. (Springer, Berlin, 2004).
 - [2] L. D. Landau and E. M. Lifshitz, Sov. Phys. JETP **5**, 512 (1957).
 - [3] E. M. Lifshitz and L. P. Pitaevskii, *Landau and Lifshitz Course of Theoretical Physics, Stat. Phys. vol 5*. (Pergamon, Oxford, 1980).
 - [4] H. Grabert, *Projection Operator Techniques in Nonequilibrium Statistical Mechanics* (Springer Berlin, Berlin, 1982).
 - [5] D. Zubarev and V. Morozov, Physica A: Statistical Mechanics and its Applications **120**, 411 (1983).
 - [6] M. Duran-Olivencia, P. Yatsyshin, B. Goddard, and S. Kalliadasis, New Journal of Physics **19** (2017), 1367-2630/aa9041.
 - [7] N. Gō, J. Stat. Phys. **30**, 413 (1983).
 - [8] P. G. de Gennes, Rev. Mod. Phys. **57**, 827 (1985).
 - [9] R. Evans, M. C. Stewart, and N. B. Wilding, Proceedings of the National Academy of Sciences **116**, 23901 (2019).
 - [10] D. Seo, A. M. Schrader, S.-Y. Chen, Y. Kaufman, T. R. Cristiani, S. H. Page, P. H. Koenig, Y. Gizaw, D. W. Lee, and J. N. Israelachvili, Proceedings of the National Academy of Sciences **115**, 8070 (2018).

- [11] D. Kashchiev, *Nucleation : basic theory with applications* (Butterworth-Heinemann, Oxford, 2000).
- [12] R. Evans, Adv. Phys. **28**, 143 (1979).
- [13] J. F. Lutsko, Adv. Chem. Phys. **144**, 1 (2010).
- [14] J. F. Lutsko, J. Chem. Phys. **135**, 161101 (2011).
- [15] J. F. Lutsko, J. Chem. Phys. **136**, 034509 (2012).
- [16] J. F. Lutsko and C. Schoonen, The Journal of Chemical Physics **161**, 104502 (2024).
- [17] J. F. Lutsko, Sci. Adv. **5**, eaav7399 (2019).
- [18] M. Duran-Olivencia, P. Yatsyshin, B. Goddard, and S. Kalliadasis, New Journal of Physics **19** (2017), 1367-2630/aa9041.
- [19] S. van Teeffelen, R. Backofen, A. Voigt, and H. Löwen, Phys. Rev. E **79**, 051404 (2009).
- [20] J. F. Lutsko and J. Lam, Phys. Rev. E **98**, 012604 (2018).
- [21] D. S. Dean, J. Phys. A: Math. Gen. **29**, L613 (1996).
- [22] K. Kawasaki, J. Stat. Phys. **93**, 527 (1998).
- [23] P.-H. Chavanis, Physica A **387**, 5716 (2008).
- [24] P. Illien, Reports on Progress in Physics **00**, 000 (2025).
- [25] J. F. Lutsko, Phys. Rev. E **102**, 062137 (2020).
- [26] J. F. Lutsko, Phys. Rev. E **105**, 034120 (2022).
- [27] D. Wales, *Energy Landscapes* (Cambridge University Press, Cambridge, 2003).
- [28] J. F. Lutsko and C. Schoonen, Phys. Rev. E **102**, 062136 (2020).
- [29] Y. Rosenfeld, Phys. Rev. Lett. **63**, 980 (1989).
- [30] R. Evans, M. Oettel, R. Roth, and G. Kahl, Journal of Physics: Condensed Matter **28**, 240401 (2016).
- [31] W. van Saarloos, D. Bedeaux, and P. Mazur, Physica A **110**, 147 (1982).
- [32] V. Hernandez, J. E. Roman, and V. Vidal, ACM Trans. Math. Software **31**, 351 (2005).
- [33] V. Hernandez, J. E. Roman, and V. Vidal, Lect. Notes Comput. Sci. **2565**, 377 (2003).
- [34] J. E. Roman, C. Campos, L. Dalcin, E. Romero, and A. Tomas, *SLEPc Users Manual*, Tech. Rep. DSIC-II/24/02 - Revision 3.19 (D. Sistemes Informàtics i Computació, Universitat Politècnica de València, 2023).
- [35] V. Hernández, J. E. Román, and A. Tomás, Parallel Comput. **33**, 521 (2007).
- [36] J. F. Lutsko, Europhys. Lett. **83**, 46007 (2008).

FLUCTUATION-DISSIPATION RELATION

Recall that

$$\begin{aligned} g(\mathbf{r}, \mathbf{r}'; [\rho_t]) &= -\nabla \cdot \rho_t(\mathbf{r}) \nabla \delta(\mathbf{r} - \mathbf{r}') \\ q_a(\mathbf{r}, \mathbf{r}'; [\rho_t]) &= \nabla_a \sqrt{2\rho_t(\mathbf{r})} \delta(\mathbf{r} - \mathbf{r}'), \end{aligned} \quad (42)$$

so

$$\begin{aligned} \int_V \sum_{a \in \{x, y, z\}} q_a(\mathbf{r}, \mathbf{r}'; [\rho_t]) q_a(\mathbf{r}'', \mathbf{r}'; [\rho_t]) d\mathbf{r}' &= \sum_{a \in \{x, y, z\}} \int_V \left\{ \nabla_a \sqrt{2\rho_t(\mathbf{r})} \delta(\mathbf{r} - \mathbf{r}') \right\} \left\{ \nabla_a'' \sqrt{2\rho_t(\mathbf{r}'')} \delta(\mathbf{r}'' - \mathbf{r}') \right\} d\mathbf{r}' \\ &= \sum_{a \in \{x, y, z\}} \nabla_a \sqrt{2\rho_t(\mathbf{r})} \nabla_a'' \sqrt{2\rho_t(\mathbf{r}'')} \int_V \delta(\mathbf{r} - \mathbf{r}') \delta(\mathbf{r}'' - \mathbf{r}') d\mathbf{r}' \\ &= \sum_{a \in \{x, y, z\}} \nabla_a \sqrt{2\rho_t(\mathbf{r})} \nabla_a'' \sqrt{2\rho_t(\mathbf{r}'')} \delta(\mathbf{r} - \mathbf{r}'') \end{aligned} \quad (43)$$

To further simplify, consider the action of this operator on an arbitrary test function, $f(\mathbf{r})$,

$$\int_V \sum_{a \in \{x, y, z\}} \nabla_a \sqrt{2\rho_t(\mathbf{r})} \left\{ \nabla_a'' \sqrt{2\rho_t(\mathbf{r}'')} \delta(\mathbf{r} - \mathbf{r}'') \right\} f(\mathbf{r}'') d\mathbf{r}'' = \sum_{a \in \{x, y, z\}} \nabla_a \sqrt{2\rho_t(\mathbf{r})} \int_V \left\{ \nabla_a'' \sqrt{2\rho_t(\mathbf{r}'')} \delta(\mathbf{r} - \mathbf{r}'') \right\} f(\mathbf{r}'') d\mathbf{r}'' \quad (44)$$

but

$$\begin{aligned} \int_V \left\{ \nabla_a'' \sqrt{2\rho_t(\mathbf{r}'')} \delta(\mathbf{r} - \mathbf{r}'') \right\} f(\mathbf{r}'') d\mathbf{r}'' &= \int_V \nabla_a'' \left\{ \sqrt{2\rho_t(\mathbf{r}'')} \delta(\mathbf{r} - \mathbf{r}'') f(\mathbf{r}'') \right\} d\mathbf{r}'' \\ &\quad - \int_V \sqrt{2\rho_t(\mathbf{r}'')} \delta(\mathbf{r} - \mathbf{r}'') \nabla_a'' f(\mathbf{r}'') d\mathbf{r}'' \end{aligned} \quad (45)$$

The first term on the right vanishes for a rectilinear integration volume with periodic boundaries or an infinite system in which everything becomes uniform at sufficiently large distance from the origin. Then,

$$\begin{aligned} \int_V \left\{ \nabla_a'' \sqrt{2\rho_t(\mathbf{r}'')} \delta(\mathbf{r} - \mathbf{r}'') \right\} f(\mathbf{r}'') d\mathbf{r}'' &= - \int_V \sqrt{2\rho_t(\mathbf{r}'')} \delta(\mathbf{r} - \mathbf{r}'') \nabla_a'' f(\mathbf{r}'') d\mathbf{r}'' \\ &= -\sqrt{2\rho_t(\mathbf{r})} \nabla_a f(\mathbf{r}) \end{aligned} \quad (46)$$

and

$$\begin{aligned} \int_V \sum_{a \in \{x, y, z\}} \nabla_a \sqrt{2\rho_t(\mathbf{r})} \left\{ \nabla_a'' \sqrt{2\rho_t(\mathbf{r}'')} \delta(\mathbf{r} - \mathbf{r}'') \right\} f(\mathbf{r}'') d\mathbf{r}'' &= -2 \nabla_a \rho_t(\mathbf{r}) \nabla_a f(\mathbf{r}) \\ &= -2 \int_V g(\mathbf{r}, \mathbf{r}''; [\rho_t]) f(\mathbf{r}'') d\mathbf{r}'' \end{aligned} \quad (47)$$

thus showing that

$$\int_V \sum_{a \in \{x, y, z\}} q_a(\mathbf{r}, \mathbf{r}'; [\rho_t]) q_a(\mathbf{r}'', \mathbf{r}'; [\rho_t]) d\mathbf{r}' = 2g(\mathbf{r}, \mathbf{r}''; [\rho_t]) \quad (48)$$

which is the fluctuation-dissipation relation.